Preprint
UCRL-JC-135120

A Real-Time Atmospheric Dispersion Modeling System

J.S. Nasstrom, G. Sugiyama, J.M. Leone, Jr. and D.L. Ermak

This article was submitted to
11th Joint Conference on the Applications of Air Pollution Meteorology with the Air and Waste Management Association
Long Beach, CA
January 9-14, 2000

U.S. Department of Energy

Lawrence
Livermore
National
Laboratory

September 29, 1999

5.1 A REAL-TIME ATMOSPHERIC DISPERSION MODELING SYSTEM

John S. Nasstrom*, Gayle Sugiyama, John M. Leone, Jr., and Donald L. Ermak
Lawrence Livermore National Laboratory, University of California
Livermore, California

1. INTRODUCTION

This paper describes a new 3-D multi-scale atmospheric dispersion modeling system and its on-going evaluation. This system is being developed for both real-time operational applications and detailed assessments of events involving atmospheric releases of hazardous material. It is part of a new, modernized Department of Energy (DOE) National Atmospheric Release Advisory Center (NARAC) emergency response computer system at Lawrence Livermore National Laboratory. This system contains coupled meteorological data assimilation and dispersion models, initial versions of which were described by Sugiyama and Chan (1998) and Leone et al. (1997). Section 2 describes the current versions of these models, emphasizing new features.

This modeling system supports cases involving both simple and complex terrain, and multiple space and time scales from the microscale to mesoscale. Therefore, several levels of verification and evaluation are required. The meteorological data assimilation and interpolation algorithms have been previously evaluated by comparison to observational data (Sugiyama and Chan, 1998). The non-divergence adjustment algorithm was tested against potential flow solutions and wind tunnel data (Chan and Sugiyama, 1997). Initial dispersion model results for a field experiment case study were shown by Leone et al. (1997). A study in which an early, prototype version of the new modeling system was evaluated and compared to the current NARAC operational models showed that the new system provides improved results (Foster et al., 1999). In Section 3, we show example results from the current versions of the models, including verification using analytic solutions to the advection-diffusion equation as well as on-going evaluation using microscale and mesoscale dispersion field experiments.

2. MODELS

The NARAC modeling system uses a continuous representation of the ground surface based on a piecewise bilinear interpolation of grid-point topographical data. This system supports run-time selection of both the number of grid points and the grid resolution, and variable resolution in both the vertical and horizontal coordinates. Variable vertical resolution provides appropriate representation of the meteorological fields in the critical near-surface region. Variable horizontal resolution is utilized when warranted by either topographical variation, metdata density, plume dimensions or source location/geometry. Nested grids can also be used to handle problems involving several spatial scales. NARAC software provides world-wide meteorological, terrain elevation and geographical data, and supports a variety of map projections for a range of spatial scales from local to global.

* Corresponding author address: John S. Nasstrom, L-103, LLNL, P.O. Box 808, Livermore, CA 94550, USA; e-mail: jnasstrom@llnl.gov

2.1 *Meteorological data assimilation*

Meteorological fields used by the dispersion model are generated by a new atmospheric data assimilation model, ADAPT (Sugiyama and Chan, 1998). ADAPT assimilates data from local observations (e.g., from surface stations, rawinsondes, profilers) and/or weather forecast models (global forecast model results obtained from meteorological centers and mesoscale model results), as well as land-surface data. The primary source of mesoscale model data is an in-house version of the Naval Research Laboratory's COAMPS model (Hodur, 1997).

ADAPT constructs meteorological fields (mean winds, pressure, precipitation, temperature, etc.). based on a variety of interpolation methods and atmospheric parameterizations. ADAPT can also diagnose turbulence quantities required by the dispersion model (see next section). Non-divergent wind fields are produced by ADAPT using an adjustment procedure based on the variational principle and a finite-element discretization. The finite element method is used for spatial discretization because of its effectiveness in treating complex terrain and its flexibility in dealing with variable resolution grids. The solution is obtained via a choice of conjugate gradient solvers using a stabilization matrix to improve computational efficiency.

2.2 *Turbulence parameterizations*

For real-time diagnostic meteorological simulations, turbulence quantities are determined using scaling relationships. The methods summarized by van Ulden and Holtslag (1985) are used to estimate turbulence scaling parameters (e.g., friction velocity, u_*; Obukhov length, L; convective velocity scale, w_*; boundary layer depth, h) using near-surface meteorological observations. A simple "slab" model is used to calculate the rate of growth of the daytime, unstable boundary layer (e.g., Tennekes, 1973).

The vertical diffusivity, K_z, in the atmospheric boundary layer (ABL) is calculated using the similarity-theory relationship

$$K_z(z) = \frac{k u_* z}{\phi_h(z/L)} e^{-4z/h} \qquad (1)$$

for $z < h$, based on that used by Lange (1989), where z is the height above ground and $\phi_h(z/L)$ is the dimensionless temperature gradient function (Dyer, 1974) typically used for scalar diffusivities. For $z > h$, K_Z is constant with height with a default value of 0.01 m^2 s^{-1}.

Horizontal velocity fluctuations often exhibit long correlation times. However, the assumptions implicit in the advection-diffusion equation used in the dispersion model are not valid until travel times much longer than the Lagrangian velocity correlation time. To compensate for this, travel-time-dependent horizontal eddy diffusivities are used. K_x and K_y are determined from the following relationship:

$$K_y = \frac{1}{2}\frac{d\sigma_y^2}{dt}. \quad (2)$$

($K_x = K_y$). The following form for σ_y proposed by Draxler (1976) is used:

$$\sigma_y = \frac{\sigma_v t}{1 + D\left(\frac{t}{T_i}\right)^{1/2}}, \quad (3)$$

where D = 0.9, σ_V is the standard deviation of the cross-wind velocity component (assumed to be equal to that for the along-wind velocity component), t is the time since the material was released at a point source, and T_i is an empirical time scale which is related to the Lagrangian correlation time of the cross-wind velocity component.

Values of σ_V are calculated using the following scaling relationship in the unstable ABL:

$$\sigma_v^2 = Au_*^2\left(1 - \frac{z}{h}\right)^{3/2} + Bw_*^2 \quad (4)$$

where A = 4.25, and B = 0.34. This relationship is derived from the work of Panofsky *et al.* (1977) and Caughey and Palmer (1979). In the stable and neutral ABL:

$$\sigma_v^2 = Au_*^2\left(1 - \frac{z}{h}\right)^{3/2} \quad (5)$$

based on the work of Nieuwstadt (1985) and Lenschow *et al.* (1988). For consistency between the stable and unstable relationships in the neutral limit, the value A = 4.25 is also used in Eq. (5). If a measured value of σ_V is available, the above parameterized σ_V relationships are scaled to match the measurement. A minimum value of σ_V = 0.5 m s^{-1} is used, which is consistent with the results of several investigators (see, e.g., Hanna and Chang, 1992). Above the boundary layer, a constant value of σ_V = 0.5 m s^{-1} is used, consistent with a very limited number of published observations (e.g., Caughey and Palmer, 1979).

For the neutral and stable ABL, the value T_i = 1000 sec proposed by Draxler (1976) is used. However, for the unstable ABL,

$$T_i = \frac{h}{\left(27u_*^3 + 1.2w_*^3\right)^{1/3}}. \quad (6)$$

This expression is based on the σ_y relationship developed by Briggs (1985) for the convective boundary layer and the approach developed by Nieuwstadt and van Duuren (1978) for interpolating between the neutral limit (w_* = 0) and convective limit ($w_* >> u_*$).

2.3 *Dispersion model*

The dispersion model, LODI, simulates the processes of mean wind advection, turbulent diffusion, radioactive decay, first-order chemical reactions, wet deposition, gravitational settling, dry deposition, and buoyant/momentum plume rise using a Lagrangian stochastic, Monte Carlo method. This model solves the 3-D advection-diffusion equation:

$$\begin{aligned}\frac{\partial C}{\partial t} &= -\bar{u}\frac{\partial C}{\partial x} - \bar{v}\frac{\partial C}{\partial y} - \bar{w}\frac{\partial C}{\partial z} \\ &+ \frac{\partial}{\partial x}\left(K_x\frac{\partial C}{\partial x}\right) + \frac{\partial}{\partial y}\left(K_y\frac{\partial C}{\partial y}\right) + \frac{\partial}{\partial z}\left(K_z\frac{\partial C}{\partial z}\right) \\ &+ w_s\frac{\partial C}{\partial z} - \Lambda C - \lambda C + Q\end{aligned} \quad (7)$$

where C is the mean air concentration of a species; $\bar{u}$, $\bar{v}$, and $\bar{w}$ are the mean wind components in the x, y, and z directions, respectively; t is time; K_x, K_y, and K_Z are the eddy diffusivities for the three coordinate directions; w_s is the absolute value of the gravitational settling velocity; Λ is the precipitation scavenging coefficient; λ is the decay constant for radioactive decay (or the rate constant for first-order chemical reaction); and Q is the source term. Additional terms are used for production of a radionuclide due to the decay of other radionuclides in a decay chain.

Equation (7) is solved using the Lagrangian stochastic, Monte Carlo method. Particle displacements due to the mean wind are calculated using the Runge-Kutta methods described by Leone et al. (1997). The displacement of a particle due to turbulent diffusion is calculated using the method developed by Ermak and Nasstrom (1999) that uses a skewed, non-Gaussian particle position probability density function.

The source term, Q, in Eq. (7) is specified using the input parameters for the initial spatial distribution of source material (options are provided for point, line, Gaussian, and uniform spherical distributions) and the total source mass (or activity) emission rate, q. Both the spatial distribution and emission rate may change in time. For an aerosol source, the mass (or activity) distribution (i.e., the mass of the species of interest as a function of particle size) can be specified with the input parameters of a lognormal distribution or from tabular input.

The dispersion model includes parameterizations for the vertical rise of bent-over plumes from continuous sources due to initial vertical momentum and/or buoyancy. Analytic expressions reviewed by Weil (1988) are used for the mean height and radius of the plume as a function of time. The final rise of a plume is limited by several factors, including the intensity of the ambient turbulence and the presence and strength of stable layers at or above the source. The model uses the minimum rise found from separate calculations of the rise due to these effects. In the absence of modeled or observed temperature data, the ambient potential temperature gradient is assumed to zero in the neutral and unstable ABL, and a similarity theory temperature profile is used in the stable ABL. The standard atmosphere temperature gradient (–0.0065 deg m^{-1}) is used above the ABL. During the initial plume rise phase of a particle trajectory, an additional mean vertical velocity due to plume rise is added to the mean vertical velocity of the particle due to other processes (mean wind, gravitational settling). Diffusion during the plume rise phase is calculated using an effective diffusivity, assuming that the standard deviation of the spatial distribution of material in the plume is proportional to the plume radius.

The terminal settling velocity, w_s, for aerosols is calculated using the particle diameter, particle density, air density, and air viscosity using methods described by Hinds (1982). The method used depends on the

Reynolds number of the flow around the falling particle. For particle Reynolds number, Re < 1, Stokes' Law is valid and is used to calculate the terminal settling velocity. For Re > 1, Stokes' Law is not valid and we use the table-based method described by Hinds (1982).

A deposition velocity, v_d, is used to parameterize the effect of all near-surface dry deposition processes below a reference height, including turbulent and molecular diffusion to the surface, inertial impaction on the surface, absorption by the surface, as well as gravitational settling. The deposition velocity for gases (w_s = 0) is $v_d = 1/r_T$, where r_T is the total deposition resistance (e.g., Wesely and Hicks, 1977). For particulate matter (w_s > 0), the deposition velocity is calculated as follows

$$v_d = \frac{w_s}{1 - e^{-w_s r_T}} \tag{8}$$

(Sehmel and Hodgson, 1978).

3. MODEL VERIFICATION AND EVALUATION

3.1 *Advection-Diffusion Equation Analytic Solutions*

A series of tests using analytic solutions were performed to verify that the dispersion model accurately solves the advection-diffusion equation. Results for solutions to the 1-D diffusion equation for linear and quadratic $K(z)$ were given previously by Ermak and Nasstrom (1999). In addition, tests were completed for the following cases for which analytic solutions are available: (1) 3-D advection and diffusion from a instantaneous Gaussian source with constant mean wind, constant diffusivities, and an impermeable lower boundary; (2) 1-D vertical diffusion of a well-mixed, uniform spatial distribution with similarity-theory $K_z(z)$ and impermeable upper and lower boundaries; (3) 3-D advection and diffusion from a continuous point source with linear $K_z(z)$, constant wind, no downwind diffusion, travel-time-dependent K_y, and impermeable lower boundary; (4) 1-D settling, surface deposition, radioactive decay, and integrated ground exposure due to a uniform vertical concentration distribution of aerosol with zero wind and zero diffusivity; (5) 2-D advection and diffusion from a continuous point source with power law $\bar{u}(z)$, linear $K_z(z)$, zero downwind diffusion, and an impermeable lower boundary. These test were used to develop automatic time step restrictions (based on grid spacing, magnitude of the diffusivity and its gradient, magnitude of the wind speed components, boundary layer depth, and decay time constant) that ensure accurate numerical solutions (less than 5% error in the computed quantities, air concentration and/or deposition, for each solution).

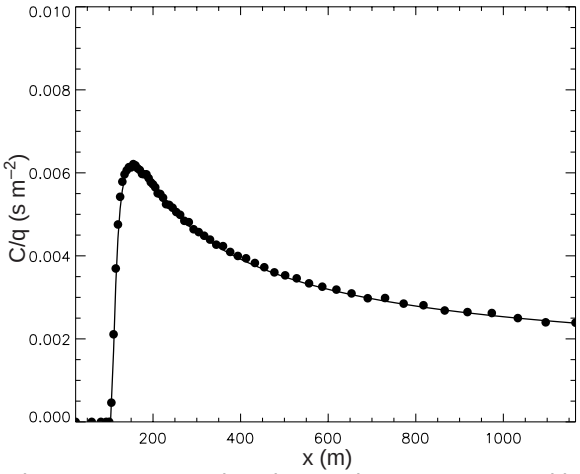

Fig. 1. Concentration (per unit source strength) versus downwind distance from analytic solution (line) and numerical model solution (circles) at 19.5 m above the surface for the 2-D case of a power law wind speed and linear diffusivity.

An example simulation result from the 2-D (downwind distance, x, versus height, z) analytic cases using a continuous point source at z=15 m, a power law $\bar{u}(z) = 5z^{0.2}$ m s^{-1}, and a linear $K_z(z) = 0.1z$ m^2 s^{-1} (both typical of the neutral surface layer) is shown in Fig. 1. In this simulation, a graded vertical wind grid was used with a minimum grid spacing of 0.25 m for the first three grid points at the surface, and each succeeding vertical level having twice the spacing of the next lower level, 10^5 particle trajectories were calculated, and concentrations were calculated by sampling particles on a grid with 3 m vertical resolution near the surface. Agreement between the numerical and analytic solutions for the mean air concentration is very good, indicating that our model can accurately simulate advection and diffusion in inhomogeneous mean wind and turbulence.

3.2 *Field Experiments*

The Project Prairie Grass experiments (Barad, 1958) were used to test the ability of our modeling system to simulate microscale dispersion. These experiments were conducted on flat, arid grassland with a continuous 10-min release of SO_2 gas at a height of 0.46 m. Time-average concentrations were measured at z = 1.5 m on arcs 50, 100, 200, 400, and 800 m from the source and at heights of 0.5, 1.0, 1.5, 2.5, 4.5, 7.5, 10.5, 13.5, and 17.5 m on six towers located in the 100-m arc. The 20-min average wind and temperature were measured at a multi-level tower instrumented at 0.25, 0.5, 1.0, 2.0, 4.0, 8.0, and 16.0 m. A rawinsonde provided upper level wind and temperature data. These observations were used by ADAPT to generate a wind field on a grid that used 26 vertical levels to resolve the tower observation levels (grid levels at z = 0, 0.25, 0.5, 1, 2, 4, 8, 16, 32, 64, … meters). A zero slip speed was imposed at the surface. In the dispersion simulation, 10^5 particle trajectories were computed and concentrations were calculated by sampling particles in a graded vertical grid with a 0.25 m vertical spacing at the surface and succeeding higher grid volumes spaced so they were centered at the heights of the concentration observations.

Two-dimensional (downwind distance versus height) simulations were made to compare model results to the crosswind-integrated 100-m arc observed concentrations computed by Wilson et al. (1981). We used values of L and u_* calculated by Wilson et al. from observed wind and temperature profiles assuming a surface roughness height of 0.005 m. Deposition velocity values were calculated using the method of Weseley and Hicks (1977) for estimating the total SO_2 deposition resistance. For the SO_2 canopy resistance, we used their value for vegetation subject to water stress, 200 s m^{-1}. For stable conditions, values of h were set to the height of the nocturnal surface-based inversion determined from the rawinsonde temperature soundings. For unstable conditions, h was set to the height of base of the elevated inversion layer in the observed temperature sounding.

Fig. 2 shows comparisons of predicted and observed crosswind-integrated concentration profiles for Prairie Grass experiments #50 (unstable), #45 (near neutral), and #59 (stable). These model results show good agreement with the observations for all three stability conditions, and demonstrate the ability of the models to simulate dispersion in the inhomogeneous mean wind and turbulence conditions found very close to the ground.

Mesoscale simulations were made of the Mesoscale Atmospheric Tracer Studies (MATS), conducted over gently rolling tree-covered terrain at the Savannah River Site in South Carolina (Weber, et al., 1992). In these experiments, SF_6 gas was released continuously for 15 min from a 61-m stack with an diameter of 2.4 m and an approximate exit velocity of 8.6 m s^{-1}. SF_6 air concentrations were sampled at ground level at distances approximately 30 km downwind of the source. A network of eight 61-m single-level meteorological towers with bi-vane anemometers and one multi-level (18, 36, 91, 137, 182, 243, and 304 m) tower with thermometers and cup anemometers provided 15-min averages of wind and temperature, and standard deviations of the wind.

In our MATS wind field simulations, the grid covered a 90 km x 90 km x 2000 m domain in the *x*, *y* and *z* directions, respectively, with 2.0 km horizontal resolution, and with a finest vertical resolution of 10 m in the grid layer nearest the ground. Wind fields were constructed at 15 min intervals based on the surface and tower observations. In these simulations, the surface layer was not completely resolved. Therefore, a logarithmic wind profile parameterization and a surface slip speed of one half the 10-m grid level wind speed were used.

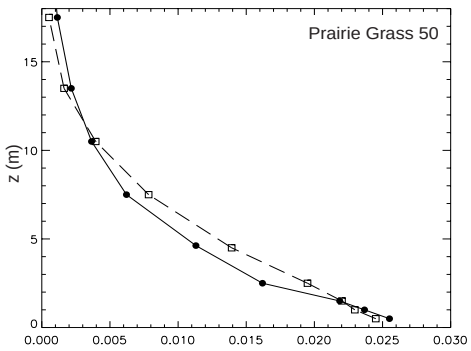

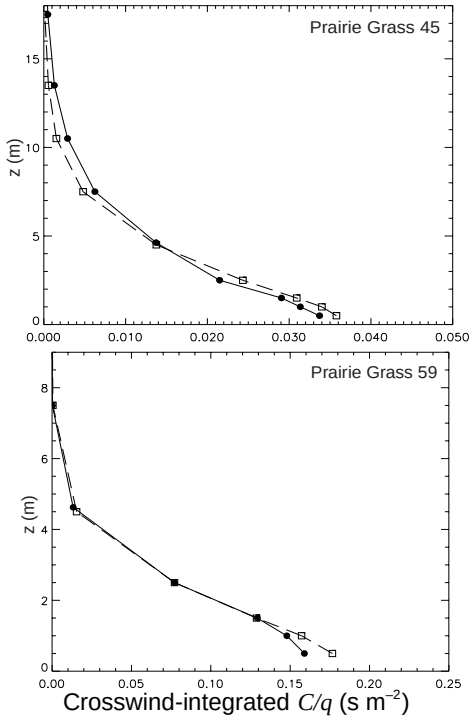

Fig. 2. Vertical profiles of predicted (circles) and observed (squares) crosswind-integrated 100-m arc air concentration (per unit source strength) for Prairie Grass experiment #50 (L = –26 m, top figure); #45 (L = –110 m, middle) and #59 (L = 7.3 m, bottom).

Surface observations of cloud cover from the nearest available station at Augusta, GA (approximately 35 km from the source location) were used to estimate the surface sensible heat flux, u_* and L, assuming a surface roughness height of 1 m, from the methods described in Section 2. For experiment #24, a temperature sounding made near the start of the SF_6 release provided an observation of the inversion height (approx. 800 m at 1612 UTC, 1112 LST). Beginning with this initial value, the growth on the convective boundary layer depth with time was calculated using the method mentioned in Section 2 and the estimates of the surface heat flux. For this simulation, the 243-m level tower data was omitted in constructing the wind field with ADAPT since it showed a obvious inconsistency compared to the other tower levels throughout the experiment. The observed cross-wind velocity variance from the 61-m tower nearest the source location were used in the model to scale the values from the cross-wind velocity variance parameterization. In our dispersion simulation, 5 x 10^4 particle trajectories were calculated, and average ground-level concentrations were calculated by sampling particles in a 0.5-km-horizontal-resolution grid with 20 m resolution in the vertical. Plume rise due to the initial vertical momentum of the source was computed, but small (5 m).

Figure 3 shows an example of a simulated 50-m AGL horizontal wind field and horizontal particle positions for MATS experiment #24 in which SF_6 was released from 1600 to 1615 UTC. Figure 4 shows a comparison of the predicted ground-level 12-min average SF_6 air concentration and the concentration observed at the line of samplers approximately 30 km downwind of the source for the time that the maximum concentration was observed at these samplers. This

comparison shows that the modeling system simulates reasonably well the crosswind spread of the concentration distribution, the north-south (*y*) position of the maximum concentration, and magnitude of the ground-level concentrations. The maximum predicted concentration has not quite reached the samplers at this time, as observed. However, at the 30 km downwind distance of the sampler line, this could be due to a small error of roughly 0.5 m s^{-1} in the average horizontal transport speed.

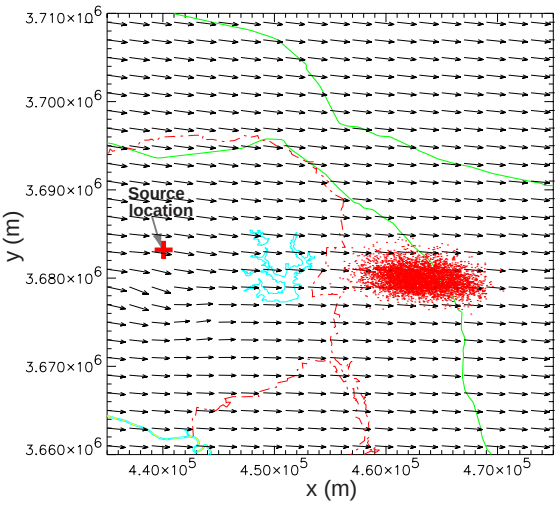

Fig. 3. Simulated 50-m AGL horizontal wind field vectors (maximum wind speed at this level is 6.2 m s^{-1}) at 16:52 UTC and (*x, y*) particle positions at 17:04 UTC for MATS experiment #24. SF_6 was released at the source location from 1600 to 1615 UTC.

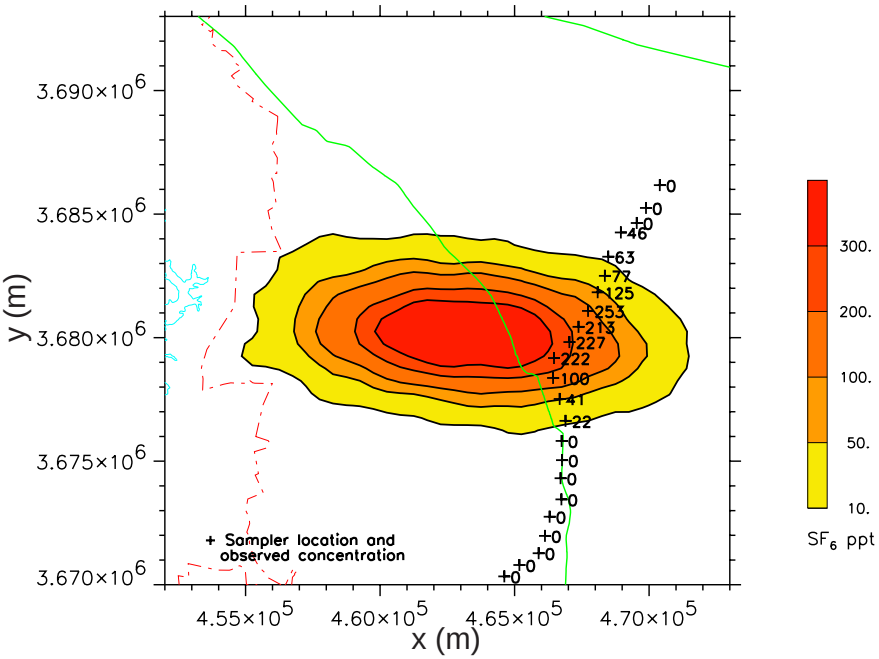

Fig. 4. Contours of predicted ground-level, average SF_6 air concentration and the observed concentrations from the line of samplers for 1701-1713 UTC in MATS experiment #24.

4. SUMMARY AND CONCLUSIONS

Results discussed above demonstrate that the numerical methods used in the new NARAC modeling system are accurate, and that transport and dispersion of tracers was generally well simulated in the microscale and mesoscale cases studied. A complete evaluation of the modeling system must obviously involve comparisons to much more experimental data, and use of a wider range of space/time, meteorological conditions, and source characteristics. This is underway using a variety of archived experimental data. The models are also being evaluated for robustness and efficiency under operational conditions. The new modeling system is scheduled to become operational at the NARAC on January 1, 2000. We are also developing urban mean wind and turbulence parameterizations, and integrating land-surface characteristic databases.

5. ACKNOWLEDGMENTS

The authors would like to express their appreciation to Denise Maddix and David Larson for their valuable contributions to the development of the dispersion model, Kevin Foster for providing field experiment data,

Hoyt Walker for the grid generation software used in this work, John Wilson (U. Alberta) for providing Prairie Grass crosswind-integrated concentrations, and Ernie Arnold for help with the map feature data. This work was performed under the auspices of the U.S. Department of Energy by the Lawrence Livermore National Laboratory under contract number W-7405-Eng-48.

6. REFERENCES

Barad, M.L., 1958: *Project Prairie Grass, A Field Program in Diffusion* (three volumes), Geophysical Research Papers No. 59, AFCRC-TR-58-235, Air Force Cambridge Research Center, U.S. Air Force, Bedford, MA.

Briggs, G.A., 1985: Analytical Parameterizations of Diffusion: The Convective Boundary Layer, *J. Clim. Appl. Meteorol.*, **24**, 1167-1186

Caughey, S.J. and S.G. Palmer (1979) Some aspects of turbulence structure through the depth of the convective boundary layer, *Quart. J. R. Met. Soc.*, **105**, 811-827.

Chan, S. and G. Sugiyama, 1997: A New Model for Generating Mass-Consistent Wind Fields over Continuous Terrain, Preprint*, ANS Sixth Topical Meeting on Emergency Preparedness and Response*, San Francisco, CA (April, 1997), 375-378

Dyer, A.J., 1974: A review of flux-profile relationships, *Bound. Layer Meteor.*, **7**, 363-72

Draxler, R.R., 1976: Determination of atmospheric diffusion parameters, *Atmos. Environ.*, **10**, 99-105.

Ermak, D.L., and J.S. Nasstrom, 1999: A Lagrangian Stochastic Diffusion Method for Inhomogeneous Turbulence, *Atmos. Environ.*, in press.

Foster, K.T., G. Sugiyama, J.S. Nasstrom, J.M. Leone, Jr., S.T. Chan, and B.M. Bowen, 1998: The use of an operational model evaluation system for model intercomparison, *Int. J. Environment and Polllution*, accepted.

Hanna, S.R. and J.C. Chang (1992) Boundary-layer parameterizations for applied dispersion modeling over urban areas, *Bound.-Layer Meteorol.*, **58**, 229-259.

Hinds, W.C., 1982: *Aerosol Technology*, John Wiley and Sons, New York, 424 pp.

Hodur, R. M. 1997: The Naval Research Laboratory's Coupled Ocean/Atmosphere Mesoscale Prediction System (COAMPS), *Mon. Wea. Rev*. **125**, 1414-1430.

Lange, R., 1989: Transferability of a Three-Dimensional Air Quality Model between Two Different Sites in Complex Terrain, *J. Appl. Meteorol.*, **28**, 7, pp. 665-679

Lenschow, D.H., X. Sheng Li, C. Juan Zhu, and B.B. Stankov (1988) The stably stratified boundary layer over the Great Plains, *Bound.-Layer Meteorol.*, **42**, 95-121.

Leone, Jr., J.M, J.S Nasstrom, and D. Maddix, 1997: A First Look at the New ARAC Dispersion Model, Preprint, *American Nuclear Society's Sixth Topical Meeting on Emergency Preparedness and Response*, San Francisco, CA, April 1997, American Nuclear Society, Inc., La Grange Park, IL.

Nieuwstadt, F.T.M. (1985) A model for the stationary, stable boundary layer, In: *Turbulence and diffusion in stable environments* (J.C.R. Hunt, ed.), pp. 149-179, Clarendon Press, Oxford.

Nieuwstadt, F.T.M. and H. van Duuren (1978) Dispersion experiments with SF_6 from the 213 m high meteorological mast at Cabauw in the Netherlands, Preprint, *Fourth Symposium on Turbulence, Diffusion, and Air Pollution*, Jan. 15-18, 1979, Reno, NV. American Meteorological Society, Boston, MA.

Panofsky, H.A., H. Tennekes, D.H. Lenschow, and J.C. Wyngaard (1977) The characteristics of turbulent velocity components in the surface layer under convective conditions. *Bound.-Layer Meteorol.*, **11**, 355-361.

Sehmel, G.A., and W.H. Hodgson, 1978: *A Model for Predicting Dry Deposition of Particles and Gases to Environmental Surfaces,* Report PNL-SA-6721, Battele Pacific Northwest Laboratories, Richland, WA.

Sugiyama, G. and S. T. Chan, 1998: A New Meteorological Data Assimilation Model for Real-Time Emergency Response, Preprint*, 10th Joint Conference on the Applications of Air Pollution Meteorology*, Phoenix, AZ (11-16 January, 1998), Am. Met. Soc., Boston, MA. 285-289

Tennekes, H., 1973: A model for the dynamics of the inversion above the convective boundary layer*, J. Atmos. Sci*., **30**, 558-567.

van Ulden, A.P. and A.A.M. Holtslag, 1985: Estimation of atmospheric boundary layer parameters for diffusion applications, *J. Climate Appl. Meteor.*, **24**, pp. 1196-1207.

Weber, A.H., S. Berman, R.J. Kurzeja, and R.P. Addis, 1992: The MATS Experiments—Mesoscale Atmospheric Transport Studies at the Savannah River Site, *Nucl. Safety*, **33**, 58-74.

Wesely, M.L. and B.B. Hicks, 1977: Some factors that affect the deposition rates of sulfur dioxide and similar gases to vegetation, *J. Air Poll. Control Assoc*., **27**, 1110-1116.

Weil, J.C., 1988: Plume Rise. In *Lectures on Air Pollution Meteorology*, A. Venkatram and J.C. Wyngaard (eds.). Am. Meteorol. Soc., Boston, 390 pp.

Wilson, J.D., G.W. Thurtell, and G.E. Kidd, 1981: Numerical simulation of particle trajectories in inhomogeneous turbulence, III: Comparison of predictions with experimental data for the atmospheric surface layer, *Bound.-Layer Meteorol.*, *21*, 443-463